

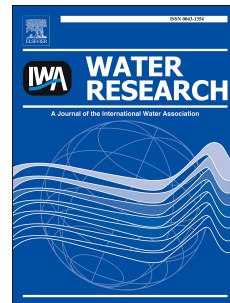
This item is the archived peer-reviewed author-version of:

Refinery and concentration of nutrients from urine with electro dialysis enabled by upstream precipitation and nitrification

Reference:

De Paepe Jolien, Lindeboom Ralph E.F., Vanoppen Marjolein, De Paepe Kim, Demey Dries, Coessens Wout, Lamaze Brigitte, Verliefde Arne R.D., Clauw aert Peter, Vlaeminck Siegfried.- Refinery and concentration of nutrients from urine with electro dialysis enabled by upstream precipitation and nitrification
Water research / International Association on Water Pollution Research - ISSN 0043-1354 - 144(2018), p. 76-86
Full text (Publisher's DOI): <https://doi.org/10.1016/J.WATRES.2018.07.016>
To cite this reference: <https://hdl.handle.net/10067/1529070151162165141>

Accepted Manuscript



Refinery and concentration of nutrients from urine with electro dialysis enabled by upstream precipitation and nitrification

Jolien De Paepe, Ralph E.F. Lindeboom, Marjolein Vanoppen, Kim De Paepe, Dries Demey, Wout Coessens, Brigitte Lamaze, Arne R.D. Verliefe, Peter Clauwaert, Siegfried E. Vlaeminck

PII: S0043-1354(18)30555-4

DOI: [10.1016/j.watres.2018.07.016](https://doi.org/10.1016/j.watres.2018.07.016)

Reference: WR 13915

To appear in: *Water Research*

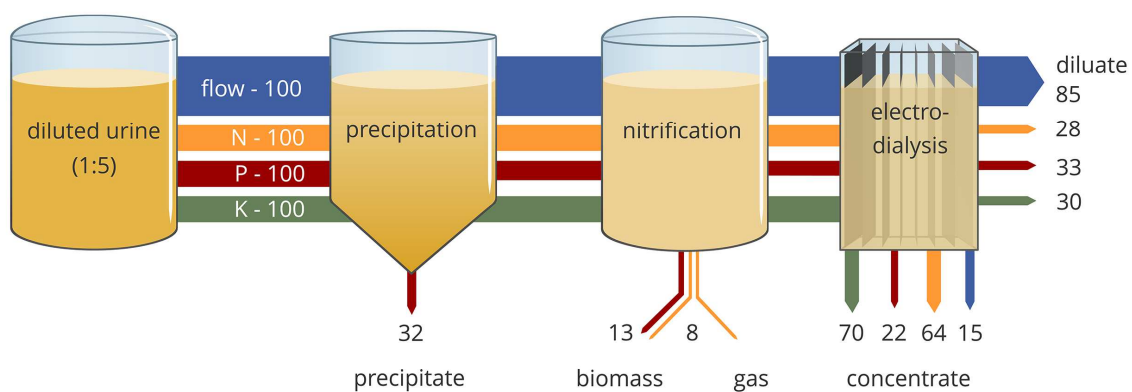
Received Date: 8 March 2018

Revised Date: 23 June 2018

Accepted Date: 6 July 2018

Please cite this article as: De Paepe, J., Lindeboom, R.E.F., Vanoppen, M., De Paepe, K., Demey, D., Coessens, W., Lamaze, B., Verliefe, A.R.D., Clauwaert, P., Vlaeminck, S.E., Refinery and concentration of nutrients from urine with electro dialysis enabled by upstream precipitation and nitrification, *Water Research* (2018), doi: 10.1016/j.watres.2018.07.016.

This is a PDF file of an unedited manuscript that has been accepted for publication. As a service to our customers we are providing this early version of the manuscript. The manuscript will undergo copyediting, typesetting, and review of the resulting proof before it is published in its final form. Please note that during the production process errors may be discovered which could affect the content, and all legal disclaimers that apply to the journal pertain.



1 **Refinery and concentration of nutrients from urine with electro dialysis enabled by**
2 **upstream precipitation and nitrification**

3 Jolien De Paep^{a,b}, Ralph E.F. Lindeboom^{a,c}, Marjolein Vanoppen^d, Kim De Paep^a, Dries Demey^e, Wout
4 Coessens^a, Brigitte Lamaze^f, Arne R.D. Verliefde^d, Peter Clauwaert^a & Siegfried E. Vlaeminck^{a,g,#}

5 ^a Center for Microbial Ecology and Technology (CMET), Faculty of Bioscience Engineering – Ghent
6 University, Coupure Links 653, 9000 Gent, Belgium

7 ^b Departament d'Enginyeria Química, Biològica i Ambiental, Escola d'Enginyeria – Universitat Autònoma de
8 Barcelona, Bellaterra 08193 Barcelona, Spain

9 ^c Section Sanitary Engineering, Department of Water Management, Faculty of Civil Engineering and
10 Geosciences – Delft University of Technology, Stevinweg 1, 2628CN, Delft, The Netherlands

11 ^d Particle and Interfacial Technology Group (PaInt), Faculty of Bioscience Engineering – Ghent University,
12 Coupure Links 653, 9000 Gent, Belgium

13 ^e QinetiQ Space, Hogenakkerhoekstraat 9, 9150 Kruibeke, Belgium

14 ^f ESA/ESTEC, Keplerlaan 1, 2200 Noordwijk, The Netherlands

15 ^g Research Group of Sustainable Energy, Air and Water Technology, Department of Bioscience Engineering –
16 University of Antwerp, Groenenborgerlaan 171, 2020 Antwerpen, Belgium

17 [#] Corresponding author: Siegfried.Vlaeminck@UGent.be;

18 Declarations of interest: none

19 **ABSTRACT**

20 Human urine is a valuable resource for nutrient recovery, given its high levels of nitrogen, phosphorus and
21 potassium, but the compositional complexity of urine presents a challenge for an energy-efficient
22 concentration and refinery of nutrients. In this study, a pilot installation combining precipitation,
23 nitrification and electrodialysis (ED), designed for one person equivalent ($1.2L_{\text{urine}} \text{ d}^{-1}$), was continuously
24 operated for ~7 months. First, NaOH addition yielded calcium and magnesium precipitation, preventing
25 scaling in ED. Second, a moving bed biofilm reactor oxidized organics, preventing downstream biofouling,
26 and yielded complete nitrification on diluted urine (20-40%, i.e. dilution factors 5 and 2.5) at an average
27 loading rate of $215 \text{ mg N L}^{-1} \text{ d}^{-1}$. Batch tests demonstrated the halotolerance of the nitrifying community,
28 with nitrification rates not affected up to an electrical conductivity of 40 mS cm^{-1} and gradually decreasing,
29 yet ongoing, activity up to 96 mS cm^{-1} at 18% of the maximum rate. Next-generation 16S rRNA gene
30 amplicon sequencing revealed that switching from a synthetic influent to real urine induced a profound
31 shift in microbial community and that the AOB community was dominated by halophilic species closely
32 related to *Nitrosomonas aestuarii* and *Nitrosomonas marina*. Third, nitrate, phosphate and potassium in
33 the filtered ($0.1 \mu\text{m}$) bioreactor effluent were concentrated by factors 4.3, 2.6 and 4.6, respectively, with
34 ED. Doubling the urine concentration from 20% to 40% further increased the ED recovery efficiency by
35 ~10%. Batch experiments at pH 6, 7 and 8 indicated a more efficient phosphate transport to the
36 concentrate at pH 7. The newly proposed three-stage strategy opens up opportunities for energy- and
37 chemical-efficient nutrient recovery from urine. Precipitation and nitrification enabled the long-term
38 continuous operation of ED on fresh urine requiring minimal maintenance, which has, to the best of our
39 knowledge, never been achieved before.

40 **Keywords:**

41 source separation, resource recovery, MBBR, MBR, electrodialysis

42 1. INTRODUCTION

43 Fertilizers are pivotal in meeting the global food demand. At present, fertilizer production mainly relies on
44 the use of non-renewable energy (to produce ammonia) and finite natural resources, such as phosphate
45 rock and potassium minerals (Ledezma et al. 2015). The growing world population, the limited resources
46 and the environmental burden of eutrophication demand a paradigm shift towards recovery and reuse of
47 nutrients (Verstraete et al. 2016). Recently, source-separated urine has gained great interest as a valuable
48 resource of nutrients, given its relatively high concentration in macronutrients ($\sim 9 \text{ g N L}^{-1}$, 0.7 g P L^{-1} and 2 g
49 K L^{-1}) (Udert et al. 2006). Efficient nutrient recovery from source-separated urine could provide an
50 estimated 20% of the nitrogen, phosphorus and potassium for the current fertilizer production in the EU
51 (Kuntke 2013, Ledezma et al. 2015). Since urine is often diluted with flushing water, it is important to
52 concentrate the nutrients in order to reduce transport and storage volumes and to facilitate the recovery of
53 nutrients (Maurer et al. 2006). Numerous technologies have been proposed to separate and/or
54 concentrate nutrients from urine. However, none of these technologies are capable of capturing the broad
55 urine nutrient spectrum in a micropollutant-free fertilizer in a scalable, energy- and chemical-efficient
56 manner. Evaporation, reverse osmosis, freeze-thawing and nitrification-distillation are energy-intensive,
57 microbial fuel cells and electrolysis cells are difficult to scale up, whereas struvite precipitation, NH_3
58 stripping and ion exchange only target specific nutrients (i.e., N or P) (Ledezma et al. 2015, Maurer et al.
59 2006, Tice and Kim 2014, Udert and Wachter 2012). In order to fill this gap, electrodialysis (ED) was
60 selected in the present study.

61 ED is a membrane separation process with an electric potential gradient as the driving force to separate
62 charged ions from an aqueous solution. Anion and cation exchange membranes compartmentalise the
63 system, producing two effluent streams, an ion-depleted diluate and ion-accumulating concentrate stream.
64 ED has been implemented at large scale ($> 20\,000 \text{ m}^3 \text{ d}^{-1}$), mostly for desalination of brackish water and
65 demineralization of industrial process water (Strathmann 2010). A few studies report on urine treatment
66 with ED for the purpose of i) water recovery (Brown et al. 1963) or urine desalination (Aponte and Colon
67 2001) in Space life support systems, ii) micropollutant removal (Escher et al. 2006) and iii) nutrient recovery

68 (Pronk et al. 2006a, Pronk et al. 2006b, Pronk et al. 2007). Operating an ED stack on urine is challenging due
69 to the high calcium and magnesium concentration and the high organic load, which can cause scaling and
70 biofouling on the membranes, and clogging of spacers and tubing. As a consequence, the reduced flux and
71 increasing resistance in the stack are limiting factors in achieving high efficiencies (Mikhaylin and Bazinet
72 2016). Thus far, autoclaved, filtered urine (Aponte and Colon 2001) or urine pre-treated with charcoal
73 adsorption (Brown et al. 1963) or microfiltration (Pronk et al. 2006a, Pronk et al. 2006b) has been used in
74 short-term ED experiments. Only one study addressed the long-term (>3 months), interrupted operation
75 (short operation times of 1-2 weeks) of an ED stack on real, hydrolysed urine (Pronk et al. 2007). The
76 desalination rate, however, decreased with approximately 50% over a period of 195 days due to fouling
77 (Pronk et al. 2007).

78 In the present study, fresh urine was used and scaling and biofouling were prevented by a combination of
79 precipitation and an aerobic bioreactor. Disadvantages of using hydrolysed urine include uncontrolled
80 precipitation of phosphorus and evaporation of ammonia during storage, leading to phosphorus and
81 nitrogen losses (Maurer et al. 2006 Udert et al. 2003b, Udert et al. 2003c). Enzymatic urea hydrolysis can be
82 prevented during storage through addition of acids, metals, caustics ..., but it is considered challenging to
83 stop the process for 100% (Randall et al. 2016, Ray et al. 2018). Calcium and magnesium were removed in a
84 precipitation reactor in which NaOH was dosed to increase the pH to 11, shifting the speciation of
85 phosphate and carbonate ions, causing supersaturation and thus triggering precipitation. Subsequently, the
86 urine was treated in an aerobic bioreactor. The purpose of the bioreactor was to i) convert biodegradable
87 organics into CO₂ and sludge by heterotrophic bacteria, thereby reducing the biofouling potential in ED, and
88 ii) to convert urea (~85% of the nitrogen in fresh urine) into nitrate through ammonification followed by
89 nitrification. In addition, nitrification decreases the pH, leading to undersaturation, thereby preventing
90 further precipitation in ED.

91 Ammonification, or the hydrolysis of urea to bicarbonate and ammonium, is initiated by the urease
92 enzyme, produced by many heterotrophic bacteria and some nitrifiers (Defoirdt et al. 2017, Koops et al.
93 1991, Mobley and Hausinger 1989). The nitrification process consists of ammonium oxidizing bacteria

94 (AOB) converting ammonium into nitrite ('nitritation') followed by the oxidation of the nitrite into nitrate
95 ('nitrataion') by nitrite oxidizing bacteria (NOB). Nitrification is a well-documented stabilisation method of
96 urine as nitrate is a stable molecule, in contrast to ammonia, which upon volatilisation causes significant
97 malodour and nitrogen losses (Coppens et al. 2016, Feng et al. 2008, Udert et al. 2003, Udert and Wachter
98 2012). Additionally, nitrate is the preferred nitrogen species for recovery as it is a charged molecule which
99 can be captured in the ED concentrate, and, in a lot of cases, the preferred nitrogen fertilizer for plants
100 (Marschner 1995).

101 The integration of precipitation, nitrification and ED to refine and concentrate nutrients from fresh urine of
102 one person equivalent was, for the first time, evaluated in an automated pilot-scale installation during four
103 months on a 20% urine solution (i.e., dilution factor of 5). As upstream precipitation and nitrification enable
104 ED to act as a key recovery stage, all units are considered equally important. The installation was operated
105 for another 40 days on a 40% urine solution (i.e., dilution factor of 2.5) to study the effect of a lower urine
106 dilution and thus a higher salinity on the nitrification and ED. The microbial community on the biofilm
107 carriers of the nitrification reactor was followed up over time through next-generation amplicon
108 sequencing of the 16S rRNA gene. To study the impact of salinity on the maximum ammonium and nitrite
109 oxidation rates of the biofilm, batch experiments were performed in which carriers were exposed to
110 salinities between 20 and 96 mS cm⁻¹. Furthermore, a batch experiment was carried out on ED to
111 investigate whether the phosphate recovery in ED was influenced by the pH of the ED feed stream. Three
112 different pH values (in the pH range of nitrification) were tested: pH 6, 7 and 8.

113 2. MATERIALS AND METHODS

114 2.1 Automated treatment train

115 Details and pictures of the equipment are provided in Figure S1-S3.

116 2.1.1 Precipitation reactor

117 Diluted human urine was dosed to the precipitation reactor based on a level control PLC (programmable
118 logic controller, Siemens Simatic HMI) feedback loop, in which detection of low level initiated pumping and
119 high level stopped pumping. The pH was controlled at 11 by dosing 2M NaOH and temperature was
120 controlled at 40°C by means of a heating and stirring plate. The content of the reactor was continuously
121 recycled (3 L h^{-1}) by a peristaltic pump to enhance the formation and growth of crystals. To prevent
122 precipitate from entering the bioreactor, urine was passed through a dead-end filter basket with glass fiber
123 cloth and two filters ($10 \mu\text{m}$ and $0.2 \mu\text{m}$).

124 2.1.2 Nitrification bioreactor

125 Nitrification and COD oxidation occurred in a moving bed biofilm reactor (MBBR) filled for 20% (v/v) with
126 polyvinyl alcohol beads and integrated in a membrane bioreactor (MBR) with an external ultrafiltration (UF)
127 module. The reactor received effluent from the precipitation reactor when the level dropped below 30.7 L.
128 The pH was controlled between 6.7 and 6.8 by dosing 2M NaOH or 1M HCl. Aeration (dissolved oxygen
129 (DO) level $>2 \text{ mg O}_2 \text{ L}^{-1}$) and mixing were provided by injection of pressurized ambient air. The UF module
130 consisted of three $0.1 \mu\text{m}$ sidestream tubular $\alpha\text{-Al}_2\text{O}_3$ membranes with a total surface area of 0.057 m^2
131 placed inside a stainless steel module and was operated at a crossflow velocity of 0.5 m s^{-1} . The UF filtrate
132 was dosed to the diluate tank of the ED unit, the UF retentate was recirculated to the bioreactor. When the
133 pressure over the UF membrane increased ($>1 \text{ bar}$), the filtration module was disconnected and cleaned by
134 recirculating a 1% P110 (alkaline) and a 1% P73 (acid) ultrasil solution (Ecolab®, MN, USA).

135 2.1.3 Electrodialysis unit

136 The ED unit contained electrolyte, diluate and concentrate tanks next to a PCell ED 64004 stack (PCA
137 GmbH, Heusweiler, Germany). The stack comprised 10 cell pairs with standard PC SA anion and PC SK
138 cation exchange membranes with an active membrane area of 64 cm^2 and 0.45 mm thick
139 silicone/polyethylene spacers (PCA GmbH, Heusweiler, Germany). The electrodes were stretched titanium,

140 coated with a mixed metal oxide platinum/iridium coating for the cathode/anode, respectively (PCA GmbH,
141 Heusweiler, Germany). A 1M NaNO₃ electrode rinsing solution was circulated in the electrode
142 compartments over the electrolyte tank. The diluate and concentrate were circulated at a constant flow
143 rate (1 L min⁻¹) between the tank and stack. The concentrate was drained when the level or the
144 conductivity in the concentrate tank exceeded the threshold (2 L or 70 mS cm⁻¹, respectively). The diluate
145 tank was continuously filled with the filtrate of the bioreactor and partially drained when the level in the
146 tank exceeded 2.1 L. The current of the power supply was controlled at 80-90% of the limiting current
147 density (LCD). The LCD was determined according to the method described by Mulder (1996) using the
148 electrical conductivity (EC) of the ED diluate. When the potential difference surmounted 10 V (about three
149 times the nominal value), the stack was cleaned in place by recirculating a 0.1% oxonia solution and a 0.01
150 M HCl solution through the diluate and concentrate compartments.

151 **2.2 Operation**

152 **2.2.1 Urine collection**

153 Urine from male donors not taking medication, was collected in a water-less urinal and stored in a freezer (-
154 20°C). Urine collection was approved by the Ethical committee of Ghent University hospital under
155 registration number B670201523246. Before feeding to the precipitation reactor, the urine was thawed
156 and preserved at 4°C. Demineralised water was added to simulate flush water. The installation was
157 operated during four months on a 20% urine solution. Daily, 1.2 L of urine and 4.6 L of demineralised water
158 were separately fed into the system and subsequently mixed in the precipitation reactor. To study the
159 effect of a higher salinity on the nitrification and the recovery efficiencies and concentration factors of the
160 ED, the installation was operated using a 40% urine solution (1.3 L d⁻¹ of urine mixed with 2.2 L d⁻¹ of
161 demineralised water) for two months.

162 **2.2.2 Reactor inoculation**

163 Based on the inoculum screening described by Coppens et al. (2016), three inoculum sources (urine
164 nitrification, OLAND and commercial aquaculture inoculum) were selected to inoculate a cultivation reactor
165 (CR), used to establish a nitrifying biofilm on the beads. The CR (22L) was operated as a moving bed biofilm

166 reactor (MBBR) and received a synthetic influent with a salinity around 10 mS cm^{-1} consisting of 0.7 g N L^{-1}
167 (as $(\text{NH}_4)_2\text{SO}_4$), $7.6 \text{ g L}^{-1} \text{ NaHCO}_3$, 25 mg P L^{-1} (as KH_2PO_4), 27 mg N L^{-1} (as NaNO_2), $104 \text{ mg COD L}^{-1}$ (as sodium
168 acetate) and $2.5 \text{ g NaCl L}^{-1}$, dissolved in tap water. Prior to operating the CR as MBBR, it was operated for
169 several months as a SBR. The initial influent composition was based on the information provided by the
170 suppliers of the inoculum and gradually tuned, also using batch assays, towards maximizing nitrification and
171 nitrification rates, while maintaining the cultures' functionality for ureolysis and COD removal at slightly
172 saline conditions. The additional nitrite was used to create a slight overcapacity in nitrification compared to
173 nitrification to minimize nitrite toxicity risks during start up. The volumetric nitrogen loading rate amounted
174 to $165 \text{ mg N L}^{-1} \text{ d}^{-1}$. The pH was between pH 6.5-8.0 (NaHCO_3 buffer) and oxygen was continuously supplied
175 with an aquarium pump ($\text{DO} > 2 \text{ mg O}_2 \text{ L}^{-1}$). An average hydraulic retention time (HRT) of 4.4 days was
176 applied to ensure sufficient selective pressure for biofilm growth by washing out the suspended biomass.
177 The bioreactor of the pilot installation was inoculated with beads from the cultivation reactor.

178 **2.2.3 Automation, operation and sampling**

179 The pilot installation was equipped with pH, DO and EC electrodes connected to an SC1000 controller
180 (Hach, CO, USA). An online ammonium analyser (AMTAX sc, Hach, CO, USA) continuously monitored the
181 ammonium concentration in the UF filtrate of the bioreactor. The process parameters were automatically
182 logged and controlled by a PLC (Siemens Simatic HMI), allowing an automated operation of the installation.
183 Additionally, samples were taken daily at different positions in the installation through sampling ports,
184 filtered over a $0.20 \mu\text{m}$ Chromafil® Xtra filter (Macherey-Nagel, PA, USA) and stored in the fridge (4°C) prior
185 to analysis. The operational conditions during the tests on a 20% and 40% urine solution are presented in
186 Table 1.

187 **TABLE 1 (double column, full width)**

188 Table 1. **Operational conditions for the precipitation reactor, nitrification bioreactor and electro dialysis**
 189 **(ED) unit during the tests on 20% and 40% urine solutions.** Average values and standard deviations are
 190 based on a period of 100 days operating using a 20% urine solution and 40 days operating using a 40%
 191 urine solution. HRT: hydraulic retention time; EC: electrical conductivity; DO: dissolved oxygen.

Urine solution [vol%]	Precipitation reactor		Nitrification bioreactor		ED diluate		ED concentrate	
	20%	40%	20%	40%	20%	40%	20%	40%
Volume [L]	0.8 - 1		30		1.8 - 2.1		0.5 - 2	
Flow rate [L d ⁻¹]	5.8	3.5	5.8	3.5	5.1	2.8	0.7	0.7
HRT [h or d]	4 h	6.8 h	5 d	8.6 d	8 h	14 h	2 - 3 d	2 - 3 d
pH [-]	10.8 ± 0.6	10.9 ± 0.2	6.7 ± 0.4	6.8 ± 0.1	6.2 ± 0.3	6.9 ± 0.2		
EC [mS cm ⁻¹]	7.6 ± 2.4	14.6 ± 2.5	10.5 ± 1.2	17.3 ± 1.1	5.1 ± 1.8	5.5 ± 0.4	43.4 ± 9.5	59.6 ± 5.8
DO [mg O ₂ L ⁻¹]			6.3 ± 2.0	5.6 ± 1.8				
Temperature [°C]	39.8 ± 6.1	40.2 ± 5.7	20.8 ± 1.3	22.3 ± 1.4	22.7 ± 2.3	22.6 ± 1.8		
Potential [V]					4.1 ± 2.1	3.9 ± 0.6		
Current [A]					0.05 ± 0.03	0.06 ± 0.01		

192

193 **2.3 Nitrification batch activity tests at different salinities**

194 To determine the salt tolerance of ureolytic bacteria, AOB and NOB on the beads, Erlenmeyer flasks were
195 filled with 200 mL beads and 300 mL mixed liquor from the bioreactor (operated using a 40% urine solution
196 and an EC around 20 mS cm⁻¹). The EC was increased by adding a salt mix (1/5 NaCl and 4/5 NaNO₃ on a
197 mass basis) to the Erlenmeyer flasks. Five different salt additions were tested: 0, 20, 40, 60 and 80 g salt L⁻¹
198 mixed liquor resulting in an EC of 20, 39, 58, 77 and 96 mS cm⁻¹. The ureolysis rate was determined by
199 adding urea (50 mg N L⁻¹) and allylthiourea (250 mg L⁻¹, to inhibit the ammonia oxidation) to the Erlenmeyer
200 flasks. AOB activity was analysed by adding 2.5 mL of urine and 0.5 g L⁻¹ NaHCO₃. NOB activity was
201 determined by spiking the flasks with NaNO₂ (50 mg N L⁻¹). The tests were performed in triplicate in a room
202 controlled at 28°C. The flasks were covered with parafilm to prevent evaporation and shaken at 130 rpm
203 using an orbital shaker (Innova® 2300, New Brunswick, The Netherlands) to provide aeration. Samples were
204 taken at a 30 minute time interval. Afterwards, they were filtered (0.20 µm Chromafil® Xtra filter,
205 Macherey-Nagel, PA, USA) and stored in the fridge. Ammonium and nitrite concentrations were
206 determined spectrophotometrically with a Tecan infinite plate reader (Infinite® F50 Absorbance Microplate
207 Reader, Tecan Trading AG, Männedorf, Switzerland) according to the Berthelot reaction (at 690 nm) and
208 Montgomery reaction (at 540 nm), respectively (Bucur et al. 2006, Montgomery and Dymock 1961). The
209 experiments lasted between 3 (at low salinity) and 24 (at high salinity) hours. Activity rates were derived
210 from the slope of the ammonium (ureolytic and AOB activity) or nitrite concentration (NOB activity) in
211 function of time. A linear model was fitted to the data in R using the 'stats' package (version 3.4.0) (R Core
212 Team 2017). Prior to formal hypothesis testing, the assumptions of homoscedasticity and normality of the
213 residuals were visually assessed and confirmed with the Bartlett test and Shapiro test in R.

214 **2.4 ED batch phosphate transport experiment**

215 A batch experiment on the ED unit was performed in order to investigate the influence of the diluate pH on
216 the phosphate transport to the concentrate. The diluate tank was filled with 2 L of UF filtrate with an EC
217 around 20 mS cm⁻¹ at the start of each experiment and the pH was adapted with HCl or NaOH to a pH of 6,
218 7 or 8. The concentrate tank was filled with 1.5 L of demineralised water. The current of the power supply
219 was automatically controlled at 90% of the LCD based on the EC of the diluate. The current, voltage, pH of

220 the diluate and conductivity of the diluate and concentrate were continuously monitored throughout the
221 experiment. Samples were taken at a 30 or 60 minute time interval, at the beginning and end of the batch
222 experiment, respectively. Afterwards, they were filtered (0.20 μm Chromafil® Xtra filter, Macherey-Nagel,
223 PA, USA) and stored in the fridge (4°C) prior to analysis. The experiments were ended after 7 h (EC diluate <
224 2.3 mS cm^{-1}).

225 **2.5 Analytical methods**

226 Chloride, nitrite, nitrate, sulphate and phosphate were analysed with anion chromatography (930 Compact
227 IC Flex with Metrosep A supp 5-150/4.0 column and conductivity detector, Metrohm, Herisau, Switzerland).
228 Sodium, total ammonium nitrogen (TAN) and potassium were measured using cation chromatography (761
229 Compact IC with Metrosep C6-250/4.0 column and conductivity detector, Metrohm, Herisau, Switzerland).
230 Calcium and magnesium concentrations were analysed by means of flame atomic absorption spectrometry
231 (Shimadzu AA-6300, Shimadzu, Kyoto, Japan). The samples were diluted and acidified with 1% nitric acid
232 and 2% of lanthanum solution. COD was determined with Nanocolor® test tubes (Nanocolor® COD 15000,
233 Macherey-Nagel, PA, USA) in unfiltered samples. Total Kjeldahl nitrogen (TKN) was analysed according to
234 Standard methods (Greenberg (1992)).

235 **2.6 Microbial community analysis**

236 Samples of the biofilm carriers from the cultivation reactor (CR) and pilot reactor (PR) were collected
237 throughout the experiment for microbial community analysis. A distinction was made between “young”
238 yellowish beads and “mature” brownish beads based on a visual colour difference. The “young” beads
239 developed their color under the autotrophic conditions of the CR and this color typically matured into
240 brownish upon several weeks exposure to the heterotrophic real urine conditions in the PR (Figure S4). The
241 beads were stored at -80°C. For each sampling time point, three beads were pooled for DNA extraction
242 using the method described by De Paepe et al. (2017). DNA extracts were sent out to LGC Genomics
243 (Teddington, UK) for library preparation and sequencing of the V3-V4 region of the 16S rRNA gene on an
244 Illumina Miseq platform. The sequence data are deposited at the NCBI (National Center for Biotechnology
245 Information) database under accession number SRP111125. The data was processed using the mothur

246 software package (v.1.38.0) (Schloss et al. 2009) as outlined by De Paepe et al. (2017) and described in
247 section 1.2 in SI.

ACCEPTED MANUSCRIPT

248 **3. RESULTS**

249 **3.1 Precipitation on a 20% urine solution**

250 To prevent scaling in the ED stack, removal of calcium and magnesium was targeted in the precipitation
251 reactor. The fivefold dilution (20% urine solution) resulted in influent concentrations of $31 \pm 10 \text{ mg Ca}^{2+} \text{ L}^{-1}$
252 and $11 \pm 5 \text{ mg Mg}^{2+} \text{ L}^{-1}$, respectively. Precipitation lowered the concentrations to $1.9 \pm 1.0 \text{ mg Ca}^{2+} \text{ L}^{-1}$ (94%
253 reduction) and $1.6 \pm 0.4 \text{ mg Mg}^{2+} \text{ L}^{-1}$ (84% reduction). Concomittantly, 32% of the phosphate and 17% of the
254 sulphate was precipitated. The sodium concentration increased threefold due to the dosage of NaOH to
255 increase the pH. The ammonium concentration increased by a factor of 2.4, indicating that some ureolysis
256 occurred in the influent tubing or in the precipitation reactor despite the high pH.

257 **3.2 Nitrification bioreactor**

258 **3.2.1 Operation using a 20% urine solution**

259 In the bioreactor, organic nitrogen and ammonium were converted into nitrate in order to stabilise the
260 urine and to be able to capture the nitrogen in a non-volatile form in ED. On average, 1.2 L d^{-1} of urine with
261 an average TKN concentration of 5.4 g N L^{-1} (before dilution) was treated, which corresponded to a
262 volumetric nitrogen loading rate of $214 \pm 85 \text{ mg N L}^{-1} \text{ d}^{-1}$. Approximately one third of the TKN was already
263 hydrolysed to ammonium before the urine entered the bioreactor (Figure 1A+B). On average 92% of the
264 nitrogen present in the influent was converted into nitrate (Figure 1A+D). Some nitrogen (<1%) was not
265 fully nitrified and was still present under the form of ammonium or nitrite in the effluent (Figure 1B+C). The
266 missing, nitrogen (<8%) was most likely lost in the precipitation reactor and the bioreactor due to struvite
267 precipitation, ammonia stripping and assimilation by the biomass, and also denitrification or N_2O
268 production could not be excluded. The time series data, presented in Figure S6, showed effluent
269 concentrations below $0.5 \text{ mg NH}_4^+ \text{-N L}^{-1}$ during 55% of the operation time and below $5 \text{ mg NH}_4^+ \text{-N L}^{-1}$ during
270 80% of the time. Only during reactor upsets (pH control failure or influent dosing problems), the
271 concentration increased above $20 \text{ mg NH}_4^+ \text{-N L}^{-1}$. Another purpose of the bioreactor was to remove the
272 organic matter in order to prevent biofouling in ED. The chemical oxygen demand (COD) in the influent and
273 effluent of the bioreactor was 818 ± 214 and $65 \pm 13 \text{ mg L}^{-1}$, respectively, which corresponds to a removal
274 percentage of 92%.

ACCEPTED MANUSCRIPT

276 3.2.2 Operation using a 40% urine solution

277 The bioreactor was operated using a 40% urine solution to study the effect of a higher salinity on the
278 nitrification. To maintain the same nitrogen loading rate of $215 \text{ mg N L}^{-1} \text{ d}^{-1}$, the total influent rate was
279 decreased from 5.8 to 3.5 L d^{-1} . As a consequence, the HRT increased from 5.0 to 8.6 days and the influent
280 concentrations of the different ions doubled compared to the test on a 20% urine solution, increasing the
281 EC in the bioreactor to $17.3 \pm 1.1 \text{ mS cm}^{-1}$ (compared to $10.5 \pm 1.2 \text{ mS cm}^{-1}$ in the test on a 20% urine
282 solution). The fraction of organic nitrogen in the influent was considerably lower compared to the period
283 on a 20% urine solution (Figure 1E), which is probably due to ureolysis as a result of the longer residence
284 time in the influent line or in the precipitation reactor. No residual ammonium or nitrite were detected in
285 the effluent of the bioreactor (Figure 1F+G), apart from accumulations on day 16 ($21 \text{ mg NO}_2^- \text{-N L}^{-1}$), day 27
286 ($62 \text{ mg NO}_2^- \text{-N L}^{-1}$) and day 28 ($16 \text{ mg NH}_4^+ \text{-N L}^{-1}$ and $89 \text{ mg NO}_2^- \text{-N L}^{-1}$) resulting from technical upsets. The
287 nitrate concentration in the effluent reached $1477 \pm 81 \text{ mg NO}_3^- \text{-N L}^{-1}$ (almost double compared to the test
288 on a 20% urine solution) (Figure 1H). Again, 91% of the COD was removed but due to the higher influent
289 concentration, the COD in the effluent was more than twice higher ($158 \text{ mg COD L}^{-1}$ instead of 65 mg COD L^{-1})
290 compared to the period on a 20% urine solution.

291 3.2.3 Halotolerance of the nitrifying biofilm

292 The short-term effect of a higher EC on maximum ureolysis, nitritation and nitrataion rates was
293 investigated in a batch experiment in which the beads were exposed to short-term salt stress by adding a
294 salt mix of NaCl and NaNO₃. The ureolysis rate decreased by 52% from $1249 \text{ mg N L}^{-1} \text{ d}^{-1}$ at an EC of 20 mS cm^{-1}
295 to $600 \text{ mg N L}^{-1} \text{ d}^{-1}$ at an EC of 96 mS cm^{-1} (Figure 2). The nitritation rate was barely affected at low EC
296 ($< 58 \text{ mS cm}^{-1}$) but decreased with 77% between an EC of 58 mS cm^{-1} and 96 mS cm^{-1} . The nitrataion
297 activity decreased almost linearly ($p=3e-8$, R^2 of 0.91) with more than 96% between 20 and 96 mS cm^{-1} . The
298 ureolysis/nitritation ratio increased whereas the nitrataion/nitritation ratio decreased at higher salt
299 concentrations. Although the NOB activity was most severely affected at high EC, nitritation remained the
300 rate limiting process.

301 FIGURE 2 (single column, no color)

302 **3.2.4 Microbial community composition**

303 The microbial community colonising the beads in the cultivation reactor (CR) and pilot reactor (PR) was
304 followed up over time through next-generation 16S rRNA gene amplicon sequencing to track the influence
305 of a synthetic urine solution *versus* the complex urine matrix. The microbial community at phylum level was
306 dominated by *Proteobacteria* ($70 \pm 10\%$) and *Bacteroidetes* ($23 \pm 9\%$), while *Acidobacteria* gradually
307 increased over time (up to 15% in the PR) (Figure S7). The most abundant families were *Moraxellaceae*,
308 *Comamonadaceae*, *Xanthomonadaceae*, *Chitinophagaceae* and the most prevalent genera included
309 *Acinetobacter*, *Luteimonas*, *Nitrosomonas* and *Comamonas* (Figure S8-S9). Approximately 30% of the
310 community could not be classified at the genus level. The most dominant OTUs (Operational Taxonomic
311 Unit) were related to *Acinetobacter venetianus* (OTU1), *Comamonas sp.* (OTU2), *Luteimonas aquatica*
312 (OTU3) and *Nitrosomonas sp.* (OTU4) (Table S2, Figure S10).

313 A principle coordinate analysis (PCoA) of the microbial community on the beads of the CR and PR at the
314 OTU level (Figure 3) revealed how the reactor-specific microbial community developed over time. After
315 start-up and stabilisation, samples originating from the same reactor (CR or PR) are clustered together. CR,
316 operated using a synthetic influent, was characterized by the dominance of *Acinetobacter*. On the other
317 hand, *Comamonas*, *Luteimonas* and *Ferruginibacter* were more characteristic for PR (Figure S9). Samples of
318 PR were more scattered and the observed shifts coincided with shifts in the influent composition, as
319 demonstrated by the arrows in Figure 3. *Acinetobacter*, *Comamonas* and *Ferruginibacter* became more
320 established on the beads when the influent was shifted from the urea solution to real urine, whereas
321 *Azoarcus* and *Dokdonella* disappeared. During operation using a 20% urine solution, the relative abundance
322 of *Luteimonas* and *Nitrosomonas* gradually increased. Changing the influent back to a synthetic $(\text{NH}_4)_2\text{SO}_4$
323 solution between the two experiments (to maintain the microbial culture), resulted in a decreased relative
324 abundance of *Acinetobacter* and further increased abundance of *Luteimonas*. Feeding the PR with a 40%
325 urine solution afterwards, led to an increased enrichment of *Comamonas* on the beads.

326 *Nitrosomonas* was the sole known AOB genus present in the CR and PR, with a total relative abundance
327 around 7%. Further classification using NCBI BLAST, RDP SeqMatch and a Maximum Likelihood phylogenetic

328 tree indicated that the key players in the AOB community were closely related to *N. aestuarii*, *N. marina*, *N.*
329 *europaea* and *N. ureae* (Table S2, Figure S11-S12). OTU4, which showed the highest sequence identity to *N.*
330 *aestuarii/marina*, was the most abundant AOB with relative abundances reaching up to 90% in some
331 samples. Interestingly, OTU24, most similar to *N. europaea*, which is only moderately halotolerant, was
332 replaced by more halophilic *N. aestuarii/marina/ureae*-like organisms in the PR when the influent was
333 shifted from a synthetic influent to real urine. When the influent was changed back to a synthetic $(\text{NH}_4)_2\text{SO}_4$
334 solution, OTU81 and OTU91 (most similar to *N. halophila* and *N. ureae*, respectively) proportionally
335 increased but disappeared when the reactor was operated again on real urine (40%).
336 158 *Bradyrhizobiaceae* (family including NOB) related OTUs were found in the microbial community, but
337 individual OTUs were <1% of the sequenced community (Figure S8). Neither qPCR gave sufficient results to
338 draw conclusions from.

339 **FIGURE 3 (single column, color)**

340 **3.3 Electrodialysis**

341 **3.3.1 Operation using a 20% urine solution**

342 The effluent of the bioreactor, with an EC of $10.5 \pm 1.2 \text{ mS cm}^{-1}$, was fed into the ED to concentrate the
343 nutrients. The predominant ions in the feed stream of the ED were sodium (of which >75% originates from
344 the NaOH dosage in the precipitation reactor and nitrification reactor), nitrate (due to nitrification),
345 chloride and potassium (Figure 4A). By applying an electric field, on average 4.1 L d^{-1} of diluate with an EC
346 of $5.1 \pm 1.8 \text{ mS cm}^{-1}$ and 0.7 L d^{-1} of concentrate with an EC around 50 mS cm^{-1} was produced. The average
347 recovery efficiencies (Figure 4C) varied between 40% and 74% with the highest efficiency for sulphate
348 (74%), followed by potassium (71%) and nitrate (70%). Only 40% of the phosphate in the feed stream was
349 transported to the concentrate stream. Sodium and nitrate made up the largest fraction of the transported
350 ions, corresponding to respectively 47% and 35% of the total molar transport, whereas phosphate and
351 sulphate contributed less than 1% to the absolute molar transport. In general, the concentrations in the
352 concentrate were 4-5 times higher than the concentrations in the feed stream (Figure 4D), while only
353 phosphate had a lower concentration factor (2.6).

354 **3.3.2 Operation using a 40% urine solution**

355 Increasing the urine concentration from a 20% to 40% urine solution, almost doubled the ion
356 concentrations and the EC of the feed stream to the ED, but the volumetric salt loading rate remained the
357 same (Figure 4B, Table S3). ED produced on average 2.8 L d⁻¹ diluate and 0.7 L d⁻¹ concentrate with an EC
358 value of around 5.5 and 60 mS cm⁻¹, respectively. The recovery efficiencies increased by 7 to 14% but the
359 concentration factors of each ion decreased (Figure 4C+D). The coulombic efficiency is compared in Table
360 S3.

361 **FIGURE 4 (double column, full width, no color)**

362 **3.3.3 Influence of pH on phosphate transport in ED**

363 The recovery efficiency of phosphate in ED was significantly lower compared to the other ions. Transfer of
364 phosphate through membranes is challenging due to its large size (high molecular mass and large hydration
365 shell resulting in a high Stokes radius) and low diffusion rate in water (Table S5). It was hypothesized that
366 the phosphate transfer to the concentrate could be enhanced by increasing the pH in the diluate since the
367 dominant phosphate species shifts from H₂PO₄⁻ to HPO₄²⁻ between a pH of 6 and 8 (Table S6). Generally, the
368 higher the charge of an ion, the more the ion is susceptible to the electric field and thus the larger the
369 driving force in the bulk solution (Nernst-Planck). This hypothesis was addressed in a batch experiment in
370 which three different pH values were tested. Since nitrate and chloride removal should not be pH
371 dependent, these ions were used as a reference to confirm whether the difference in recovery efficiency of
372 phosphate could be attributed to the pH difference and not to technical variability between the tests.
373 Phosphate transfer was clearly influenced by the pH as opposed to nitrate and chloride transfer (Figure 5,
374 S14). After an electric charge of 2500 Coulomb (C) had passed through the ED, 29%, 54% and 31% of
375 phosphate was removed from the diluate at a pH of 6, 7 and 8, respectively, yielding pH 7 as optimum.

376 **FIGURE 5 (single column, no color)**

377 **3.4 Recovery of N, P and K**

378 The aim of this study was to determine the recovery potential of the nutrients in urine based on the
379 performance of the pilot installation. During operation using a 20% urine solution, on average 32% of the
380 phosphate-P was captured in precipitates. In total, 64% of the nitrogen, 22% of the phosphorus and 70% of

381 the potassium were captured in the concentrate. On average, 29% of the nitrogen, 33% of the phosphorus
382 and 30% of the potassium remained in the diluate (Figure 6A-C, S13). About 8% of the nitrogen was not
383 recovered, as mentioned in Section 3.2.1. The concentrate contained on average 3.7 g $\text{NO}_3^- \text{-N L}^{-1}$, 1.5 g $\text{K}^+ \text{L}^{-1}$
384 ¹ and 0.06 g $\text{PO}_4^{3-} \text{-P L}^{-1}$. On a 40% urine solution, 29% of the phosphate-P was captured in precipitates. In
385 total, 70% of the nitrogen, 38% of the phosphate-P and 83% of the potassium were captured in the
386 concentrate. On average, 17% of the nitrogen, 32% of the phosphate-P and 17% of the potassium remained
387 in the diluate (Figure 6D-F). About 13% of the nitrogen was lost. The concentrate contained on average 5.1
388 g $\text{NO}_3^- \text{-N L}^{-1}$, 2.3 g $\text{K}^+ \text{L}^{-1}$ and 0.06 g $\text{PO}_4^{3-} \text{-P L}^{-1}$.

389 **FIGURE 6 (single column, no color)**

390 4. DISCUSSION

391 4.1 Precipitation and nitrification minimize scaling and biofouling in ED

392 In this study, an integrated system combining precipitation, nitrification and ED was evaluated to refine and
393 concentrate nutrients from fresh urine. Operation of this three-stage system was successfully
394 demonstrated in a relevant environment, corresponding to level 6 on the technology readiness level (TRL)
395 scale. The use of a precipitation reactor proved to be an effective strategy to safeguard the ED from
396 excessive scaling. More than 90% of the calcium and 80% of the magnesium was precipitated and no scaling
397 was observed in the ED unit. Both the precipitation and nitrification reactor require base addition. In the
398 precipitation reactor, approximately 215 mmol NaOH L⁻¹ urine was dosed in the precipitation reactor to
399 increase the pH to 11. In the nitrification reactor, base is needed to counteract the acidification caused by
400 nitrification. Without base addition, maximally ~50% of the nitrogen in urine can be converted into nitrate
401 (Udert et al. 2003a). In principle, base addition in the precipitation reactor does not increase the total base
402 consumption, as a more alkaline influent entering the bioreactor reduces the amount of alkaline
403 equivalents required in the bioreactor to counteract the acidification. In total, about 300 mmol NaOH L⁻¹
404 urine was needed to convert all urea into nitrate, of which only one third was dosed in the nitrification
405 reactor.

406 The use of a bioreactor proved to be an effective strategy to limit biofouling in ED by oxidizing the COD.
407 Moreover, uncharged urea was converted into nitrate in order to stabilise the urine and to capture the
408 nitrogen in a non-volatile form in ED. Although the total nitrogen concentration in the influent fluctuated
409 due to the variable composition of urine, stable nitrification was achieved in the bioreactor with an average
410 volumetric nitrogen loading rate of 215 mg N L⁻¹_{reactor} d⁻¹, and a salinity of 10.5 mS cm⁻¹. Only after reactor
411 disturbances (due to failure of the pH control or influent dosing problems), ammonium was detected in the
412 bioreactor effluent. Nitrifiers quickly recovered once the optimal conditions were restored. Bacteria grown
413 in a biofilm are generally more protected to transient stressors, such as a low pH and high free ammonia
414 concentration due to diffusion limitations (Ikuma 2013). Moreover, nitrification, which causes the
415 acidification, is generally hampered by a low pH, presumably due to a limited ATP generation (Fumasoli et
416 al. 2015). In addition, besides precipitation and protection of the subsequent ED, the precipitation reactor

417 was also used to increase the alkalinity of the nitrification reactor influent. As a consequence, we never
418 observed the pH dropping below 5.5, in case of pH control failure. It is in this respect also noteworthy that
419 the cultivation reactor was pH controlled solely by providing sufficient alkalinity in the feed and not by a
420 pH-controller.

421 ED was used to concentrate nutrients in an energy-efficient manner. The concentrate flow was generated
422 by osmotic and electro-osmotic water transport across the membrane and contained about 70% of the ions
423 of the feed stream. The increase in concentrate EC and obtained concentration factors of 3-5 are in line
424 with results obtained by Pronk et al. (2007). Periodic cleaning in place (~once a month) with an acid and
425 alkaline solution was sufficient to keep the ED stack operational >7 months with the same membranes and
426 a stable performance. Such cleaning can easily be automated. However, the anion exchange membranes
427 turned brown (Figure S15), which was also reported by Aponte and Colon (2001). This is probably due to
428 irreversible adsorption of negatively charged organic molecules (Aponte and Colon 2001).

429 **4.2 Nitrification and COD oxidation remained unaffected at a decreased urine dilution**

430 The high salt content of urine and base addition leads to a high EC in the bioreactor. Living in a salty
431 environment is an energetically costly process for bacteria since more energy is required to balance the cell
432 osmotic pressure (Oren 1999). This limits the energy available for nitrification, which typically results in
433 lower activity rates at high EC. The salt tolerance of the nitrifying community on the beads was assessed in
434 a batch experiment in which beads were exposed to a short-term salt shock. The maximum ureolysis,
435 nitritation and nitrataion rates of the beads decreased with 52%, 82% and 96%, respectively, when the EC
436 was increased from 20 mS cm⁻¹ to 96 mS cm⁻¹. Interestingly, the rate limiting nitritation and hence, the
437 overall nitrification rate, remained unaffected up to 40 mS cm⁻¹. This also explains why nitrification was not
438 affected during continuous operation using a 40% urine solution, despite the higher EC (17.3 mS cm⁻¹
439 instead of 10.5 mS cm⁻¹). The results of the batch experiment suggest that the bioreactor can operate on
440 undiluted urine (expected EC between 45-60 mS cm⁻¹) but at a lower volumetric rate, although this should
441 be tested on the long-term. The relatively high salt resistance of the beads is probably a result of the
442 inoculum selection (Coppens et al. 2016). The higher drop in nitrataion rate indicates that the NOB on the
443 beads were more sensitive to the short-term salt stress than the AOB. Literature is inconclusive concerning

444 the salt tolerance of AOB *versus* NOB, due to differences in experimental set-up, operational conditions and
445 test duration, salt dosage and AOB and NOB community composition (Moussa et al. 2006). Moussa et al.
446 (2006) and Coppens et al. (2016) reported that AOB were more sensitive to salt stress. On the other hand,
447 Bassin et al. (2011), Dincer and Kargi (1999), Cui et al. (2009) and Cortes-Lorenzo et al. (2015) concluded,
448 based on the accumulation of nitrite in their experiments, that NOB were more affected by salinity.

449 **4.3 Shifts in microbial community composition parallel shifts in influent composition**

450 The shifts in microbial community composition in the pilot reactor coincided with changes in the influent
451 composition, as shown by PCoA analysis (Figure 3) and may be attributed to the nature of the organic
452 fraction in the influent (acetate in synthetic medium *versus* complex COD matrix in urine). In addition,
453 salinity is known to affect the microbial community composition in nitrification reactors (Bassin et al. 2012,
454 Coppens et al. 2016, Cortes-Lorenzo et al. 2015, Gonzalez-Silva 2016, Moussa et al. 2006). Classification
455 using NCBI BLAST, RDP SeqMatch and a maximum likelihood phylogenetic tree indicated that the AOB
456 community was dominated by species closely related to *N. aestuarii* or *N. marina*. Both species are obligate
457 halophilic and described in marine environments (Koops et al. 1991). *N. aestuarii* was also found to be the
458 dominating AOB species in reactors operated on seawater (Gonzalez-Silva 2016, Sudarno et al. 2010). The
459 presence of these halophilic AOB species can also explain why the nitrification activity was so well preserved
460 at high EC in the batch experiment. Besides salinity, the shifts in the AOB community in the pilot reactor
461 corresponded to the nitrogen source (urea-N or ammonium-N). OTUs related to the urease-negative *N.*
462 *europaea* and *N. halophila* (Koops et al. 1991), only thrived when the reactor was operated using a
463 synthetic ammonium sulphate solution.

464 **4.4 Lowering the urine dilution leads to a higher recovery efficiency but a lower concentration factor in**

465 **ED**

466 Increasing the urine concentration (from 20% to 40%), decreased the volume ratio of diluate to concentrate
467 from 5.8 to 4. Due to the higher EC gradient between the diluate and concentrate and the increased
468 transport of ions from diluate to concentrate, the osmotic and electro-osmotic water transport increased.
469 Hence, relatively more concentrate was produced on a 40% urine solution. Depending on the ion, the
470 recovery efficiency increased by 7 to 14%, which is probably due to the higher residence time in the diluate

471 tank (14h instead of 8h). Despite the higher end concentrations and overall EC of the concentrate on a 40%
472 urine solution, the concentration factors decreased, as a result of the higher ion concentrations in the feed
473 stream. To conclude, more nutrients were captured in the concentrate, but in a comparatively larger
474 concentrate volume.

475 **4.5 Strategies to increase nutrient recovery efficiencies**

476 Respectively 70% and 80% of the ions were captured in 15% and 20% of the initial volume when the pilot
477 installation was operated using a 20% or 40% urine solution. It is almost impossible to capture all nutrients
478 in the concentrate. As a result of the equilibrium established between the diluate and concentrate stream,
479 part of the nutrients remain in the diluate. Additionally, relatively low concentration factors (ion
480 concentration in the concentrate stream divided by the concentration in the feed stream) present a
481 second limitation inherent to ED due to the osmotic and electro-osmotic water transport. A high
482 concentration gradient between the diluate and the concentrate, leads to increased osmotic water
483 transport from diluate to concentrate and back diffusion of ions from concentrate to diluate, which in turn
484 limits the maximum achievable concentration factor.

485 In case of phosphate, the large size and low diffusion rate of the ion limits the recovery efficiency to 40%,
486 as opposed to 70%-75% for all other ions, corresponding to a concentration factor of only 2.6. It was
487 hypothesized that the phosphate transport would increase by increasing the pH in the diluate since more
488 phosphate ions are dissociated at a higher pH, which could facilitate the transport, as the ions are more
489 susceptible to the electric field. The recovery efficiency of phosphate in the batch test at pH 7 was indeed
490 higher compared to pH 6. The slower phosphate transport at pH 8 compared to pH 7 can possibly be
491 attributed to competition in migration with carbonate ions. Like phosphate, the charge of carbonate
492 depends on the pH. Most of the carbonate is uncharged (H_2CO_3) at pH 6 while more than 90% of the
493 carbonate species have a charge of -1 (HCO_3^-) at pH 8 (Table S7). Further research is needed to confirm the
494 hypothesis of reduced phosphorus transport due to carbonate competition at elevated pH.

495 Another way to recover more phosphorus, is to precipitate all the phosphorus in the precipitation reactor.
496 Phosphorus precipitation is limited by calcium and magnesium due to the excess of anions (phosphate,
497 sulphate and carbonate) in urine. By substituting NaOH by $\text{Ca}(\text{OH})_2$ or $\text{Mg}(\text{OH})_2$ to increase the pH in the

498 precipitation reactor or adding another calcium or magnesium source, up to 90% of the phosphate can be
499 precipitated (Etter et al. 2011). However, excess calcium or magnesium dosage should be avoided to
500 prevent scaling issues in the ED unit.

501 Decreasing the concentrate volume by means of distillation is an option to concentrate the nutrients in a
502 smaller volume. Distillation was already applied by Udert and Wachter (2012) in combination with
503 nitrification to concentrate nutrients in urine. All nutrients were recovered in a dry solid. However, the high
504 energy demand of distillation ($\sim 700 \text{ Wh}_{\text{primary energy}} \text{ L}^{-1} \text{ urine}$) presents a major drawback of the process. The
505 energy consumption of ED is significantly lower. The electrode power consumption of ED in this study
506 equalled only $4.3 \text{ Wh}_{\text{electrical energy}} \text{ L}^{-1} \text{ urine}$ or $14 \text{ Wh}_{\text{primary energy}} \text{ L}^{-1} \text{ urine}$ (Table S4). However, ED removed only
507 $\sim 88\%$ of the water, whereas distillation can remove almost all water. Udert and Wachter (2012) suggested
508 that the energy demand could be significantly reduced by first removing 80% of the water with reverse
509 osmosis and subsequently operating distillation with vapor compression ($\sim 100 \text{ Wh L}^{-1} \text{ urine}$). Alternatively,
510 the required 80% water removal could be obtained by ED instead of RO, as demonstrated in this study. To
511 conclude, a combination of precipitation, nitrification, ED and distillation could offer a maximal
512 concentration of nutrients with a minimal input of energy.

513 **4.6 Resource reuse possibilities for precipitate, ED concentrate and ED diluate**

514 The output of the integrated system consists of the precipitates formed in the precipitation reactor and the
515 diluate and concentrate stream of the ED unit. The precipitates could be used as a solid phosphorus
516 fertilizer in agriculture. About 30% of the phosphate in urine was incorporated in the precipitates, which
517 corresponds to values reported in literature (Udert et al. 2006). The use of urine derived precipitates as
518 fertilizer has been demonstrated by Bonvin et al. (2015). Moreover, it was reported by Escher et al. (2006)
519 and Ronteltap et al. (2007) that urine precipitates were clean and safe fertilizers since the micropollutants
520 in urine (pharmaceuticals, hormones...) mainly remained in the liquid phase.

521 The ED concentrate is rich in nutrients, predominantly nitrogen (NPK = 85.9/0.7/13.4 mole%), which is
522 present under the form of nitrate. Nitrate, in contrast to urea, ammonia or ammonium nitrate, is a
523 thermally stable, non-volatile molecule and, in a lot of cases, the preferred nitrogen source for plants
524 (Marschner 1995, Udert and Wachter 2012). Besides nitrogen, plant growth requirements are also met for

525 potassium whereas phosphorus will be the limiting macronutrient in the ED concentrate due to the partial
526 incorporation in the precipitates (Larsen et al. 2013). The excessive salt concentration, particularly sodium,
527 resulting from the NaOH demand by precipitation and nitrification, might present another barrier for
528 fertilizer application. In this regards, partial nitrification is a promising new lead to reduce the sodium load,
529 simultaneously saving chemicals (Udert and Wachter 2012). The dense nature of the ED membranes
530 typically results in a high retention of pathogens and micropollutants in the diluate (Escher et al. 2006,
531 Pronk et al. 2006b, Pronk and Kone 2009). However, Pronk et al. (2006a) showed that breakthrough of
532 certain micropollutants (e.g., propranolol and ibuprofen) can occur over time. To guarantee a
533 micropollutant-free product, a post-treatment, such as ozonation or adsorption on activated carbon, can be
534 included to remove the residual micropollutants in the concentrate (Dodd et al. 2008, Larsen et al. 2013,
535 Pronk et al. 2007, Udert et al. 2016). Ozonation is even more effective in combination with a nitrate based,
536 COD low stream given the ozone scavenging potential of ammonium and competition between COD and
537 micropollutants for the chemical oxidant (Larsen et al. 2013, Pronk et al. 2007).

538 Finally, the ED diluate is low in nutrients and salts, which makes it a suitable stream for water recovery
539 through membrane filtration, as particularly relevant for regenerative life support systems for human Space
540 exploration (Clauwaert et al. 2017, Lindeboom et al. 2015).

541 **5. CONCLUSION**

- 542 • An electrodialysis (ED) stack was operated for ~7 months on real, diluted urine. The use of a
543 precipitation reactor and aerobic bioreactor proved to be an effective strategy to minimize scaling
544 and biofouling in ED.
- 545 • More than 90% and 95% of incoming COD and urea were converted in the bioreactor at salinities of
546 10 to 20 mS cm⁻¹. Shifts in the microbial community coincided with changes in the influent
547 composition of the bioreactor. The AOB community was dominated by species closely related to
548 *Nitrosomonas aestuarii* and *Nitrosomonas marina*.
- 549 • Respectively 70% and 80% of the ions were captured in 15% and 20% of the initial volume when
550 the pilot installation was operated using a 20% or 40% urine solution.
- 551 • The P-rich precipitates and N+K-rich ED concentrate can be valorised as fertilizers, whereas water
552 can be recovered from the ED diluate. Further research on the fate of micropollutants and
553 pathogens in the three-stage system is necessary to valorise the recovered fertilizers

554 6. ACKNOWLEDGEMENTS

555 This article has been made possible through the authors' involvement in the MELiSSA project, ESA's life
556 support system research program

557 (http://www.esa.int/Our_Activities/Space_Engineering_Technology/Melissa).

558 The authors would like to acknowledge

559 i) the financial support of the Belgian Federal Science Policy Office (BELSPO) [grant-ID

560 4000109518/13/NL/JC, project title: Water Treatment Unit Breadboard, managed by ESA],

561 ii) the MELiSSA foundation to support JDP via the POMP1 (Pool Of MELiSSA PhD) program,

562 iii) the Research Foundation Flanders (FWO, grant-ID: IWT130028, title: SBO BRANDING) and the

563 SpecialResearch Fund (BOF) Concerted Research Actions (GOA, BOF12/GOA/008) from the Flemish

564 Government to support KDP,

565 iv) IEC N.V. for building the installation,

566 v) Avecom and dr. Kai Udert from EAWAG for providing the ABIL sludge and the urine nitrification biomass,

567 respectively,

568 vi) Tim Lacoere for designing the graphical abstract.

569 7. SUPPLEMENTARY INFORMATION

570 Supplementary information related to this article can be found at [http link].

8. REFERENCES

- 572 Aponte, V.M., Colon, G., 2001. Sodium chloride removal from urine via a six-compartment ED cell for use in
573 Advanced Life Support Systems (Part 2: Limiting current density behavior). *Desalination* 140 (2), 133-144.
- 574 Bassin, J.P., Kleerebezem, R., Muyzer, G., Rosado, A.S., van Loosdrecht, M.C.M., Dezotti, M., 2012. Effect of
575 different salt adaptation strategies on the microbial diversity, activity, and settling of nitrifying sludge in
576 sequencing batch reactors. *Applied Microbiology and Biotechnology* 93 (3), 1281-1294.
- 577 Bassin, J.P., Pronk, M., Muyzer, G., Kleerebezem, R., Dezotti, M., van Loosdrecht, M.C.M., 2011. Effect of
578 Elevated Salt Concentrations on the Aerobic Granular Sludge Process: Linking Microbial Activity with
579 Microbial Community Structure. *Applied and Environmental Microbiology* 77 (22), 7942-7953.
- 580 Bonvin, C., Etter, B., Udert, K.M., Frossard, E., Nanzer, S., Tamburini, F., Oberson, A., 2015. Plant uptake of
581 phosphorus and nitrogen recycled from synthetic source-separated urine. *Ambio* 44, S217-S227.
- 582 Brown, D.L., Lindstrom, R.W., Smith, J.D., 1963. The recovery of water from urine by membrane
583 electrodialysis. U.S. Air Force Medical Research Laboratory, AMRL-TDR-63, 56.
- 584 Bucur, B., Icardo, M.C., Calatayud, J.M., 2006. Spectrophotometric determination of ammonium by an rFIA
585 assembly. *Revue Roumaine De Chimie* 51 (2), 101-108.
- 586 Clauwaert, P., Muys, M., Alloul, A., De Paepe, J., Luther, A., Sun, X.Y., Ilgrande, C., Christiaens, M.E.R., Hu,
587 X.N., Zhang, D.D., Lindeboom, R.E.F., Sas, B., Rabaey, K., Boon, N., Ronsse, F., Geelen, D., Vlaeminck, S.E.,
588 2017. Nitrogen cycling in Bioregenerative Life Support Systems: Challenges for waste refinery and food
589 production processes. *Progress in Aerospace Sciences* 91, 87-98.
- 590 Coppens, J., Lindeboom, R., Muys, M., Coessens, W., Alloul, A., Meerbergen, K., Lievens, B., Clauwaert, P.,
591 Boon, N., Vlaeminck, S.E., 2016. Nitrification and microalgae cultivation for two-stage biological nutrient
592 valorization from source separated urine. *Bioresource Technology* 211, 41-50.
- 593 Cortes-Lorenzo, C., Rodriguez-Diaz, M., Sijkema, D., Juarez-Jimenez, B., Rodelas, B., Smidt, H., Gonzalez-
594 Lopez, J., 2015. Effect of salinity on nitrification efficiency and structure of ammonia-oxidizing bacterial
595 communities in a submerged fixed bed bioreactor. *Chemical Engineering Journal* 266, 233-240.
- 596 Cui, Y.W., Peng, C.Y., Peng, Y.Z., Ye, L., 2009. Effects of Salt on Microbial Populations and Treatment
597 Performance in Purifying Saline Sewage Using the MUCT Process. *Clean-Soil Air Water* 37 (8), 649-656.
- 598 De Paepe, K., Kerckhof, F.-M., Verspreet, J., Courtin, C.M., Van de Wiele, T., 2017. Inter-individual
599 differences determine the outcome of wheat bran colonization by the human gut microbiome.
600 *Environmental Microbiology* 19 (8), 3251-3267.
- 601 Defoirdt, T., Vlaeminck, S.E., Sun, X.Y., Boon, N., Clauwaert, P., 2017. Ureolytic Activity and Its Regulation in
602 *Vibrio campbellii* and *Vibrio harveyi* in Relation to Nitrogen Recovery from Human Urine. *Environmental*
603 *Science & Technology* 51 (22), 13335-13343.
- 604 Dincer, A.R., Kargi, F., 1999. Salt inhibition of nitrification and denitrification in saline wastewater.
605 *Environmental Technology* 20 (11), 1147-1153.
- 606 Dodd, M.C., Zuleeg, S., Von Gunten, U., Pronk, W., 2008. Ozonation of Source-Separated Urine for Resource
607 Recovery and Waste Minimization: Process Modeling, Reaction Chemistry, and Operational Considerations.
608 *Environmental Science & Technology* 42 (24), 9329-9337.
- 609 Escher, B.I., Pronk, W., Suter, M.J.F., Maurer, M., 2006. Monitoring the removal efficiency of
610 pharmaceuticals and hormones in different treatment processes of source-separated urine with bioassays.
611 *Environmental Science & Technology* 40 (16), 5095-5101.
- 612 Etter, B., Tilley, E., Khadka, R., Udert, K.M., 2011. Low-cost struvite production using source-separated urine
613 in Nepal. *Water Research* 45 (2), 852-862.
- 614 Feng, D.L., Wu, Z.C., Xu, S.H., 2008. Nitrification of human urine for its stabilization and nutrient recycling.
615 *Bioresource Technology* 99 (14), 6299-6304.
- 616 Fumasoli, A., Morgenroth, E., Udert, K.M., 2015. Modeling the low pH limit of *Nitrosomonas eutropha* in
617 high-strength nitrogen wastewaters. *Water Research* 83, 161-170.
- 618 Gonzalez-Silva, B.M., 2016. Salinity as a driver for microbial community structure in reactors for nitrification
619 and anammox. Thesis for the Degree of Philosophiae Doctor, Norwegian University of Science and
620 Technology-Trondheim, Norway.

- 621 Greenberg, A.E., Clesceri, L.S. and Eaton, A.D., 1992. Standard Methods for the Examination of Water and
622 Wastewater. 18th edition. American Public Health Association (APHA) / American Water Works Association
623 (AWWA) / Water Environment Federation. Washington DC, USA.
- 624 Ikuma, K., Decho, A. W. & Lau, B. L.T., 2013. The Extracellular Bastions of Bacteria - A Biofilm Way of Life.
625 Nature Education Knowledge 4(2):2.
- 626 Koops, H.P., Bottcher, B., Moller, U.C., Pommereningroser, A., Stehr, G., 1991. Classification of 8 new
627 species of ammonia-oxidizing bacteria - *Nitrosomonas communis* sp. nov., *Nitrosomonas ureae* sp. nov.,
628 *Nitrosomonas aestuarii* sp. nov., *Nitrosomonas marina* sp. nov., *Nitrosomonas nitrosa* sp. nov.,
629 *Nitrosomonas eutropha* sp. nov., *Nitrosomonas oligotropha* sp. nov. and *Nitrosomonas halophila* sp. nov.
630 Journal of General Microbiology 137, 1689-1699.
- 631 Kuntke, P., 2013. Nutrient and energy recovery from urine, PhD thesis, Wageningen University,
632 Wageningen, The Netherlands.
- 633 Larsen, T.A., Udert, K.M., Lienert, J., 2013. Source separation and decentralization for wastewater
634 management. IWA Publishing.
- 635 Ledezma, P., Kuntke, P., Buisman, C.J.N., Keller, J., Freguia, S., 2015. Source-separated urine opens golden
636 opportunities for microbial electrochemical technologies. Trends in Biotechnology 33 (4), 214-220.
- 637 Lindeboom, R.E.F., Alonso Farinas, B., Clauwaert, P., Vanoppen, M., Christiaens, M., Abbas, A., Coessens W.,
638 De Paepe, J., Beckers, H., Dotremont, C., Rabaey, K., Verliefde, A.R.D., Lamaze B., Demey, D.a.V., S.E., 2015.
639 Water and nutrient recovery from urine and grey water in Space. Abstract, 1st IWA Resource Recovery
640 Conference, Ghent, Belgium.
- 641 Marschner, H., 1995. Mineral nutrition of higher plants. 2nd edition, London : Academic, c1995.
- 642 Maurer, M., Pronk, W., Larsen, T.A., 2006. Treatment processes for source-separated urine. Water
643 Research 40 (17), 3151-3166.
- 644 Mikhaylin, S., Bazinet, L., 2016. Fouling on ion-exchange membranes: Classification, characterization and
645 strategies of prevention and control. Advances in Colloid and Interface Science 229, 34-56.
- 646 Mobley, H.L.T., Hausinger, R.P., 1989. Microbial ureases - significance, regulation, and molecular
647 characterization. Microbiological Reviews 53 (1), 85-108.
- 648 Montgomery, H.A.C., Dymock, J.F., 1961. The determination of nitrite in water. Analyst 86, 414-416.
- 649 Moussa, M.S., Sumanasekera, D.U., Ibrahim, S.H., Lubberding, H.J., Hooijmans, C.M., Gijzen, H.J., van
650 Loosdrecht, M.C.M., 2006. Long term effects of salt on activity, population structure and floc characteristics
651 in enriched bacterial cultures of nitrifiers. Water Research 40 (7), 1377-1388.
- 652 Mulder, M., 1996. Basic Principles of Membrane Technology. Second edition, Kluwer Academic Publishers,
653 the Netherlands.
- 654 Oren, A., 1999. Bioenergetic aspects of halophilism. Microbiology and Molecular Biology Reviews 63 (2),
655 334-348.
- 656 Pronk, W., Biebow, M., Boller, M., 2006a. Electrodialysis for recovering salts from a urine solution
657 containing micropollutants. Environmental Science & Technology 40 (7), 2414-2420.
- 658 Pronk, W., Biebow, M., Boller, P., 2006b. Treatment of source-separated urine by a combination of bipolar
659 electrodialysis and a gas transfer membrane. Water Science and Technology 53 (3), 139-146.
- 660 Pronk, W., Kone, D., 2009. Options for urine treatment in developing countries. Desalination 248 (1-3), 360-
661 368.
- 662 Pronk, W., Zuleeg, S., Lienert, J., Escher, B., Koller, M., Berner, A., Koch, G., Boller, M., 2007. Pilot
663 experiments with electrodialysis and ozonation for the production of a fertiliser from urine. Water Science
664 and Technology 56 (5), 219-227.
- 665 R Core Team, 2017. R: A language and environment for statistical computing. R Foundation for Statistical
666 Computing, Vienna, Austria. <https://www.R-project.org/>.
- 667 Ronteltap, M., Maurer, M., Gujer, W., 2007. The behaviour of pharmaceuticals and heavy metals during
668 struvite precipitation in urine. Water Research 41 (9), 1859-1868.
- 669 Schloss, P.D., Westcott, S.L., Ryabin, T., Hall, J.R., Hartmann, M., Hollister, E.B., Lesniewski, R.A., Oakley,
670 B.B., Parks, D.H., Robinson, C.J., Sahl, J.W., Stres, B., Thallinger, G.G., Van Horn, D.J., Weber, C.F., 2009.
671 Introducing mothur: Open-Source, Platform-Independent, Community-Supported Software for Describing
672 and Comparing Microbial Communities. Applied and Environmental Microbiology 75 (23), 7537-7541.

- 673 Strathmann, H., 2010. Electrodialysis, a mature technology with a multitude of new applications.
674 Desalination 264 (3), 268-288.
- 675 Sudarno, U., Bathe, S., Winter, J., Gallert, C., 2010. Nitrification in fixed-bed reactors treating saline
676 wastewater. Applied Microbiology and Biotechnology 85 (6), 2017-2030.
- 677 Tice, R.C., Kim, Y., 2014. Energy efficient reconcentration of diluted human urine using ion exchange
678 membranes in bioelectrochemical systems. Water Research 64, 61-72.
- 679 Udert, K.M., Etter, B., Gounden, T., 2016. Promoting Sanitation in South Africa through Nutrient Recovery
680 from Urine. Gaia-Ecological Perspectives for Science and Society 25 (3), 194-196.
- 681 Udert, K.M., Fux, C., Munster, M., Larsen, T.A., Siegrist, H., Gujer, W., 2003. Nitrification and autotrophic
682 denitrification of source-separated urine. Water Science and Technology 48 (1), 119-130.
- 683 Udert, K.M., Larsen, T.A., Gujer, W., 2006. Fate of major compounds in source-separated urine. Water
684 Science and Technology 54 (11-12), 413-420.
- 685 Udert, K.M., Wachter, M., 2012. Complete nutrient recovery from source-separated urine by nitrification
686 and distillation. Water Research 46 (2), 453-464.
- 687 Verstraete, W., Clauwaert, P., Vlaeminck, S.E., 2016. Used water and nutrients: Recovery perspectives in a
688 'panta rhei' context. Bioresource Technology 215, 199-208.

689

690

691 **FIGURE CAPTIONS**

692 **Figure 1. Nitrogen concentrations in the influent and effluent of the bioreactor on 20% and 40% urine**

693 **solutions.** Total nitrogen (TN) is calculated as the sum of total Kjeldahl nitrogen (TKN), NO_2^- -N and NO_3^- -N.

694 Organic N is calculated by subtracting NH_4^+ -N from TKN. Inorganic N equals the sum of NH_4^+ -N, NO_2^- -N and

695 NO_3^- -N. Samples were analysed over a period of 100 days on a 20% urine solution (n=35) and over a period

696 of 40 days on a 40% urine solution (n=16). The box-and-whisker plots depict the minimum, first quartile,

697 median, third quartile, maximum and outlying points ($>1.5 \times$ interquartile range).

698 **Figure 2. Maximum ureolysis, nitritation and nitratation rates and ratios as a function of electrical**

699 **conductivity (EC).** The error bars display the standard deviation (n=3).

700 **Figure 3. Principle coordinate analysis (PCoA) biplot of the microbial community composition on the**

701 **beads in the cultivation reactor (CR) and pilot reactor (PR) at the OTU level, based on the Jaccard**

702 **distances as determined by next-generation 16S rRNA gene amplicon sequencing.** Each sample is

703 indicated by a symbol with a shape according to the reactor and bead and a colour according to the influent

704 composition. A visual distinction was made between mature and young beads based on the difference in

705 colour of the beads (Figure S4). The numbers (1-10) correspond to the sampling day (day 1, 37, 72, 86, 100,

706 114, 135, 156, 218 and 259). Day 1 refers to the day of the first sample, corresponding to, respectively, 150

707 and 1 days after start-up of CR and PR.

708 **Figure 4. Performance of the electro dialysis (ED) unit on 20% and 40% urine solutions.**
709 Each plot displays average values and standard deviations, based on 35 samples over 100 days using a 20%
710 urine solution and 16 samples over 40 days operating using a 40% urine solution.

711 **A) Concentration in the ED influent and diluate during operation using a 20% urine solution.**

712 **B) Concentration in the ED influent and diluate during operation using a 40% urine solution.**

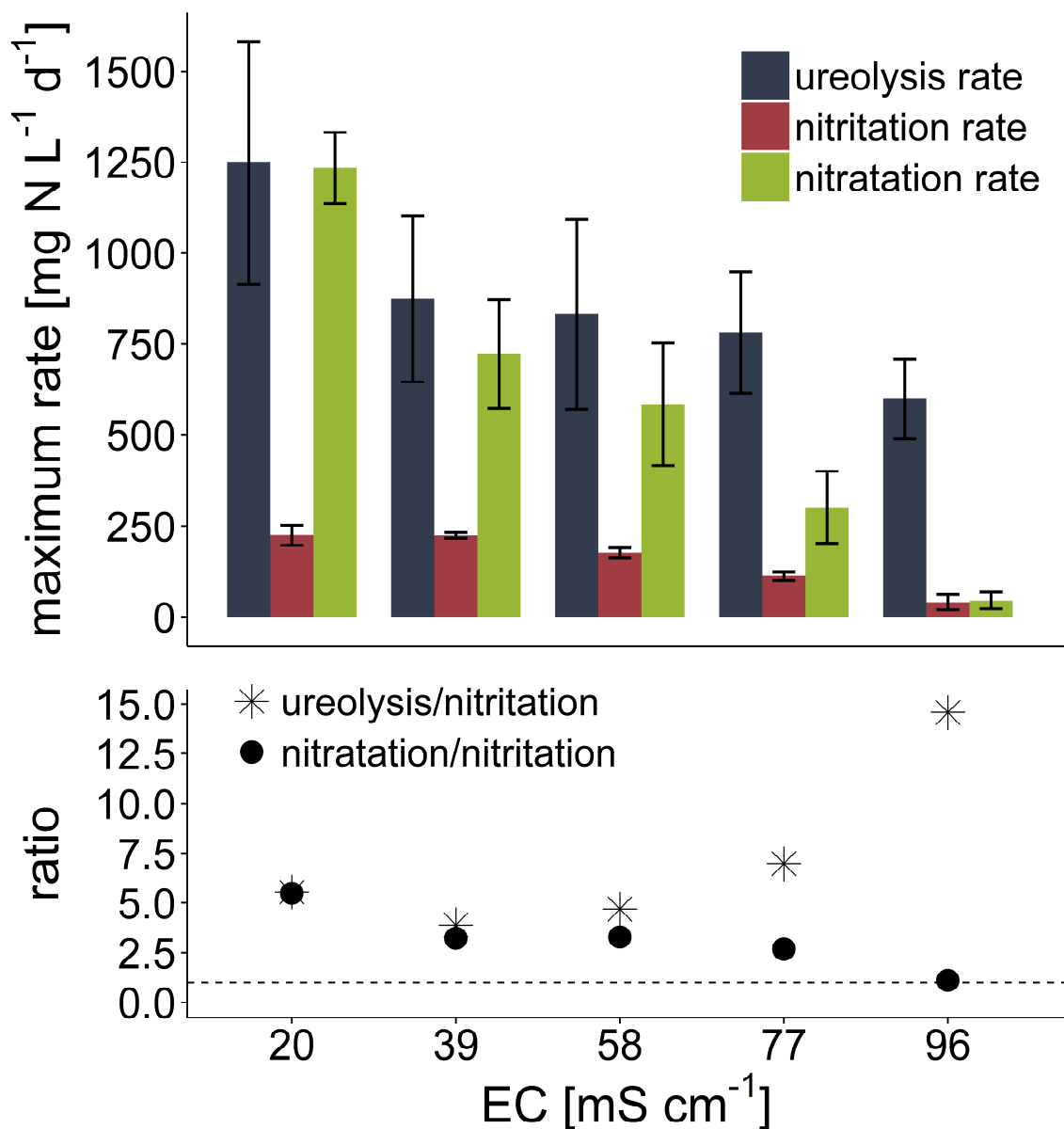
713 **C) Recovery efficiency, calculated by dividing the difference in mass of an ion between the feed stream**
714 **(ED influent) and diluate by the mass of the ion in the feed stream.**

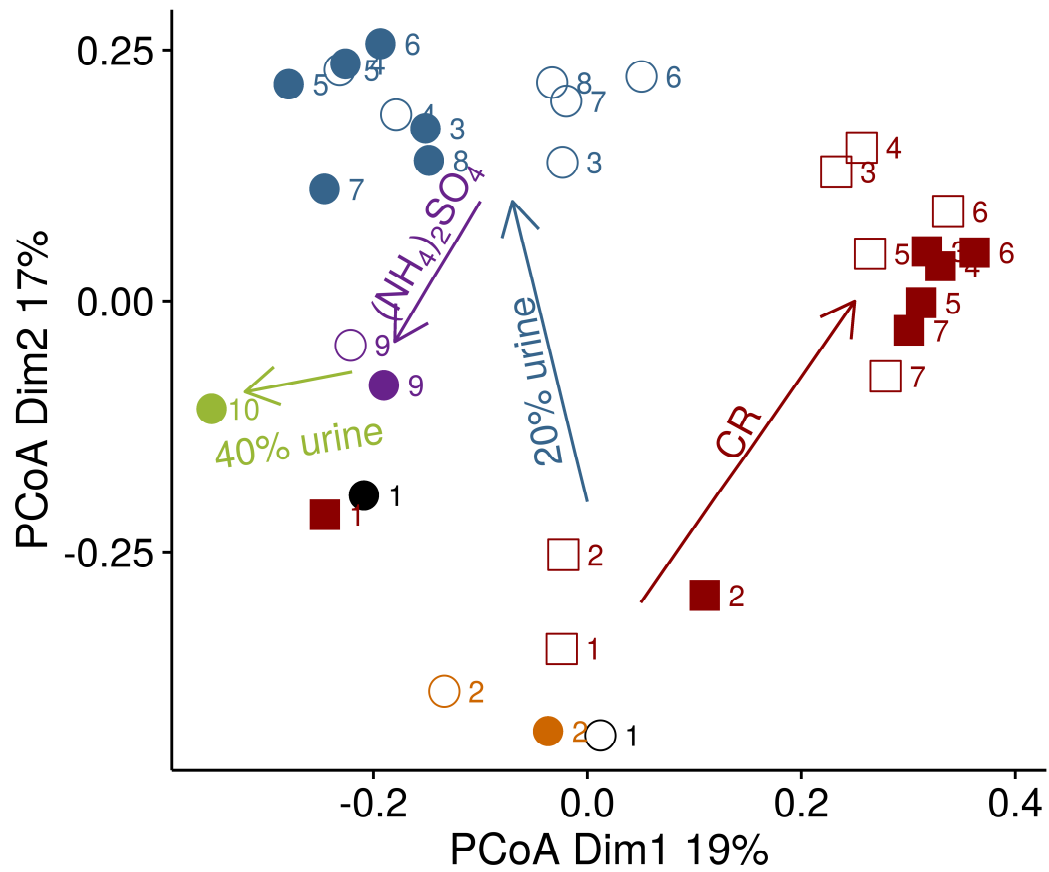
715 **D) Concentration factor, calculated by dividing the ion concentration in the concentrate stream by the**
716 **concentration in the feed stream (ED influent).**

717 **Figure 5. Recovery efficiency of phosphate in function of the cumulative electric charge that passed**
718 **through the stack in the ED batch experiment at pH 6, 7 and 8.** The cumulative electric charge (in
719 Coulomb) was calculated by multiplying the applied current and time ($Q_{i+1}=Q_i + I_{i+1}*(t_{i+1}-t_i)$). The recovery
720 efficiency was calculated by dividing the difference in phosphate concentration in the diluate at time t and
721 t_0 by the phosphate concentration at t_0 .

722 **Figure 6. Nitrogen, phosphorus and potassium concentration in the different stages of the pilot**
723 **installation during operation using 20% and 40% urine solutions.** Samples were analysed over a period of
724 100 days on a 20% urine solution (n=35) and over a period of 40 days on a 40% urine solution (n=16). The
725 nitrogen concentration in the influent is calculated as the sum of total Kjeldahl nitrogen (TKN), NO_2^- -N and
726 NO_3^- -N concentrations. The nitrogen concentration after nitrification, in the diluate and concentrate is the
727 sum of NH_4^+ -N, NO_2^- -N and NO_3^- -N.

ACCEPTED MANUSCRIPT

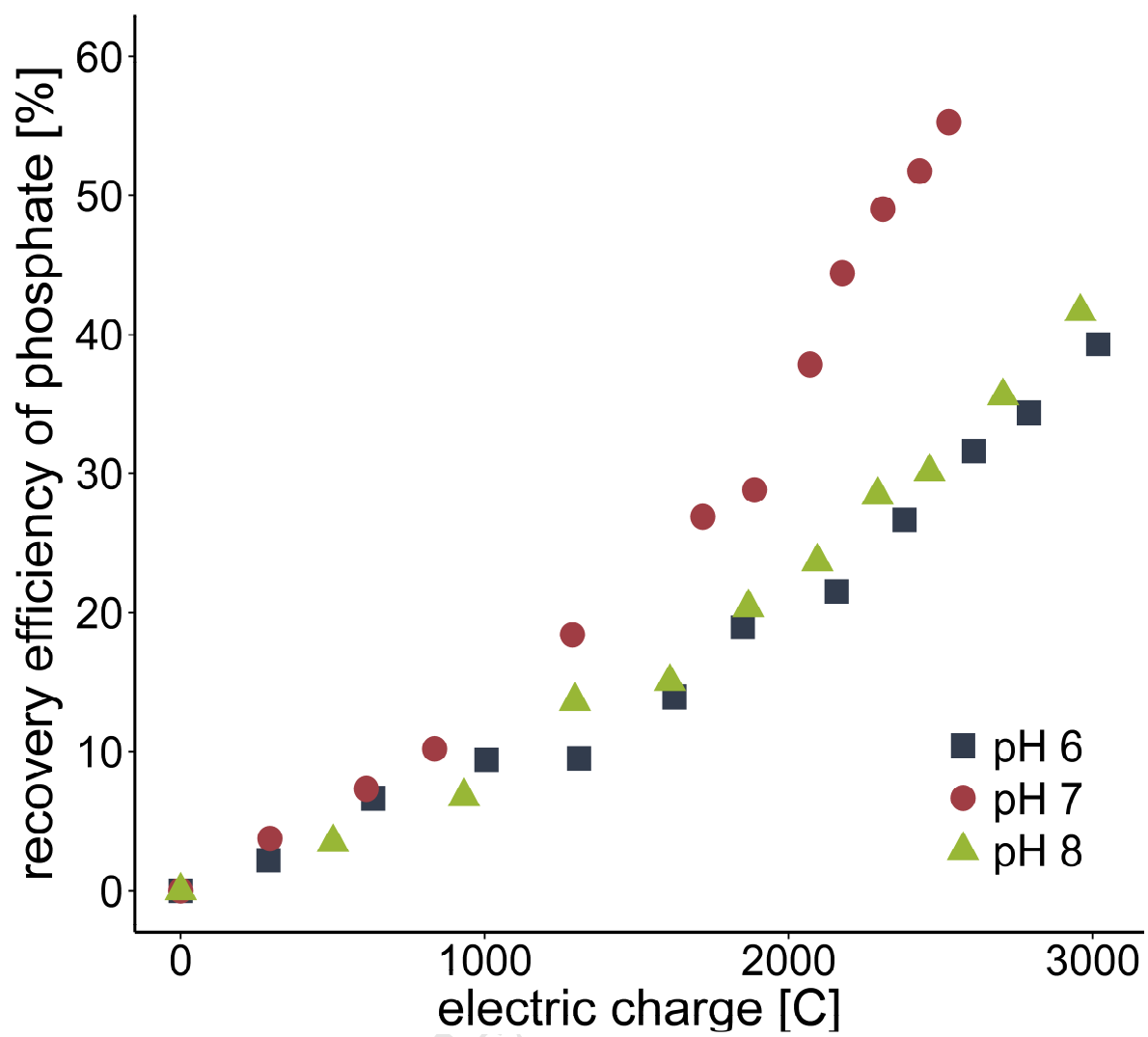




Reactor CR_young beads PR_young beads
 CR_mature beads PR_mature beads

Influent $(\text{NH}_4)_2\text{SO}_4$ 20% urine 40% urine
 urea solution $(\text{NH}_4)_2\text{SO}_4$ CR_ $(\text{NH}_4)_2\text{SO}_4$

ACCEPTED MANUSCRIPT



ACCEPTED MANUSCRIPT

HIGHLIGHTS

1. Pre-treatment enables ED operation on real urine with minimal scaling & biofouling
2. 64-70% of N, 54-67% of P, 70-83% of K was captured in 15-20% of the initial volume
3. Base dosage for precipitation equally lowered base demand for full nitrification
4. More than 90% and 95% of incoming COD and urea were converted at 10-20 mS cm⁻¹
5. Nitrifying sludge cultivated at 10 mS cm⁻¹ still demonstrated activity >90 mS cm⁻¹